coatings

MDPI

*Article*

# Effect of Sintering Temperature on Tensile Properties of Ti-6Al-4V Alloy Manufactured Through Metal Injection Molding

**Zhengyang Mai [1], Haiying Wang [2], Yongjun Su [1,*], Changjiang Zhang [3,*], Yigao Miao [1], Chuancang Zhou [1] and Lili Xu [1]**

[1] School of Engineering, Lishui University, Lishui 323000, China; 17857861144@163.com (Z.M.); miao@lsu.edu.cn (Y.M.); zhouchuancang@163.com (C.Z.); 17858963494@163.com (L.X.)
[2] Jiangsu Jinwu New Materials Co., Ltd., Taizhou 225300, China; haiying.wang@jsjinwu.com
[3] College of Materials Science and Engineering, Taiyuan University of Technology, Taiyuan 030024, China
* Correspondence: suyongjun2009@163.com (Y.S.); zhangchangjiang@tyut.edu.cn (C.Z.)

**Abstract:** Titanium and titanium alloys exhibit low density, high strength and excellent corrosion resistance, and have become workhorses in modern aerospace and chemical processing industries. Recently, Ti-6Al-4V alloy has been manufactured through metal injection molding (MIM). MIM is widely utilized in various manufacturing industries due to the near-net-forming process, especially in the preparation of difficult-to-deform high-temperature alloys. Sintering temperature is vital to ensuring good tensile mechanical properties. In this work, Ti-6Al-4V alloy was sintered under various sintering temperatures, from 1150 to 1250 °C. The effect of sintering temperature on the mechanical properties was evaluated. The tensile test results exhibited that a yield strength of 896.35 MPa, an ultimate tensile strength of 980.83 MPa and plastic elongation of 9.61% were produced at 1150 °C for 4 h; a yield strength of 877.23 MPa, an ultimate tensile strength of 981.92 MPa and plastic elongation of 7.74% were produced at 1200 °C for 4 h; and a yield strength of 923.33 MPa, an ultimate tensile strength of 1002.24 MPa and plastic elongation of 6.57% were produced at 1250 °C for 4 h.

**Keywords:** metal injection molding (MIM); Ti-6Al-4V alloy; sintering temperatures; tensile properties

check for updates

Academic Editor: Aivaras Kareiva

Received: 14 November 2024
Revised: 8 December 2024
Accepted: 12 December 2024
Published: 25 December 2024

**Citation:** Mai, Z.; Wang, H.; Su, Y.; Zhang, C.; Miao, Y.; Zhou, C.; Xu, L. Effect of Sintering Temperature on Tensile Properties of Ti-6Al-4V Alloy Manufactured Through Metal Injection Molding. *Coatings* **2025**, *15*, 8. https://doi.org/10.3390/coatings15010008

**Copyright:** © 2024 by the authors. Licensee MDPI, Basel, Switzerland. This article is an open access article distributed under the terms and conditions of the Creative Commons Attribution (CC BY) license (https://creativecommons.org/licenses/by/4.0/).

## 1. Introduction

Titanium and titanium alloys are widely used in the manufacturing of some key components in the aerospace, weaponry and marine fields, and in the chemical industry and medical treatment, due to their high specific strength, low density, unrivaled corrosion resistance and good oxidation resistance at relatively high temperatures, which can effectively improve the safety and reliability of engineering equipment [1–5]. Titanium and titanium alloys are relatively expensive materials, and their traditional processing, such as machining and casting, greatly increases their cost [6]. In addition, owing to poor workability, it is difficult to use them to produce parts with complicated shapes. Therefore, in the processing of titanium and titanium alloys, near-net-shape technology has played an important role [7,8]. Metal injection molding (MIM) is suitable for the large-scale production of small and complex-shaped titanium and titanium alloy parts [9–13], as it combines the versatility and high productivity of plastic injection molding with the sintered powder metallurgy technique [14,15]. This method with low production costs has attracted widespread attention in the metal industry due to its near-net-shape technology and high material utilization. [16–18]. In recent years, MIM has become an advanced processing method

for the low-cost production of complex-shaped titanium and titanium alloy parts [19,20]. During this process, the feedstock is obtained by mixing titanium powder with suitable binders. After mixing, the feedstock is injected into a mold through an injection molding machine. Then, the binders are extracted from the molded parts during the debinding process. Finally, the debound part is sintered at an appropriate temperature, for a suitable duration and in an appropriate atmosphere to obtain parts with acceptable mechanical and physical properties [21]. In high-performance structural applications, titanium alloys composed of α and β structures are usually suitable. The most commonly used alloy in this category is Ti-6Al-4V, accounting for 50% of the total usage of titanium alloys. This alloy is highly favored due to its outstanding workability and overall mechanical properties.

As mentioned earlier, a typical MIM process consists of four processing steps: feedstock formulation (formulating binders), injection molding, debinding and sintering [22]. Nowadays, some researchers focus mainly on formulating binders through metal injection molding. Choosing the appropriate binder system is crucial for the success of MIM technology. This is because the performance of the binder can affect the distribution of metal particles, the forming process and the final performance of the sintered parts [18]. Ferri et al. selected a wax-based binder composed of 60 wt.% paraffin, 35 wt.% ethyl acetate and 5 wt.% stearic acid to prepare Ti-6Al-4V alloy with a tensile strength of 800 MPa and an elongation of 15% [23]. Guo et al. utilized a binder composed of 63 wt.% paraffin wax, 12 wt.% polyethylene glycol, 14 wt.% polyethylene, 10 wt.% polypropylene and 1 wt.% stearic acid homogenized with Ti-6Al-4V alloy powder for injection molding [24]. A critical loading of 72 vol.% was obtained by the feedstock based on the binder. However, sintering temperature is the most influential on the properties of MIMed titanium alloys [25]. Ergül and Özkan sintered Ti-6Al-4V alloy under vacuum at different temperatures and for different durations [12]. The maximum ultimate tensile strength was obtained at 1275 °C for 10 h. Mohamad Nor et al. optimized the sintering parameter to prepare Ti-6Al-4V alloy [26]. They found that a tensile strength of 934.33 MPa could be attained when Ti-6Al-4V was sintered at 1200 °C for 1 h, but no information on elongation was given. Obasi et al. found that the maximum temperature is important in terms of the tensile strength of Ti-6Al-4V alloy [27]. They prepared Ti-6Al-4V alloy with yield strength of more than 750 MPa, UTS of more than 860 MPa and plastic elongation of about 14.3% when the maximum temperature was 1350 °C. Wang and Shi used a wax-based binder composed of 1 wt.% stearic acid, 35 wt.% low-density polyethylene and 60 wt.% paraffin wax homogenized with Ti-6Al-4V alloy powder for injection molding [28]. The authors found that the viscosity of the raw material decreased with the extension of mixing time but increased with an increase in powder loading when studying its rheological properties. However, only a few people studied the effect of sintering temperatures on the mechanical properties and microstructure of injection-molded Ti-6Al-4V alloy.

Therefore, in the present study, the effect of sintering temperature on the relative sintered density, microstructure characteristics and mechanical properties of Ti-6Al-4V alloy prepared through MIM was systematically investigated. Three sintering temperatures of 1150 °C, 1200 °C and 1250 °C were employed.

## 2. Materials and Methods

Pre-alloyed Ti-6Al-4V powders with a spherical morphology (Figure 1), purchased from Jiangsu Jinwu New Material Co., Ltd. (Taizhou, China), were used as usable raw material for MIM manufacturing in this study. The particle size and the distribution pattern of the powder were studied using a particle size analyzer in a dispersion medium used at 36 °C and 49% ethylene glycol. Table 1 shows the distribution of particle size. The powder had an average size of 24.26 μm. The initial impurity content provided by the supplier (as

shown in Table 2) was relatively low in the Ti-6Al-4V alloys. The binder system consisted of 4 wt.% of polypropylene (PP), 85 wt.% polyoxymethylene (POM), 6 wt.% of polyethylene (PE), 1.5 wt.% paraffin wax (PW), 3 wt.% ethylene vinyl acetate copolymer (EVA) and 0.5 wt.% stearic acid (SA). These ingredients were used as the main carriers, surfactants, thickeners and shrinking agents. We mixed the powder binder in a Z-shaped blade mixer at a temperature of 175 °C for one hour to produce feedstock of 65 vol.% powder loading of titanium powders. Successively, we lowered the temperature and removed the mixture and cut it into a small granular size of around 3–4 mm. Thermal gravimetric analysis (TGA) was performed on an SDT Q600 thermogravimetric analyzer (TA Instruments, New Castle, DE, USA) at a heating rate of 2 °C/min under an flow rate of 100 mL/min in an argon atmosphere to evaluate the thermal debinding behavior of the polymers for the Ti-MIM process. The temperature range was 27 °C to 630 °C. Figure 2 shows a DSC-TGA curve for the feedstock prepared from Ti-6Al-4V powders. There were two clear endothermic processes. The first-stage interval was 153.6 °C–170.5 °C with the peak at 161.3 °C. The second-stage interval was 317.6–363.1 °C with the peak at 319.1 °C. There were two distinct stages of mass changes in the TGA curve. The first stage ranged from 249.2 °C to 396.6 °C. About 80 wt.% of the binder was decomposed in this temperature range. The second stage ranged from 396.6 °C to 449.6 °C, and about 94 wt.% of the binder was decomposed in this temperature range, leaving pristine Ti-6Al-4V powders and a small amount of binder. The decomposition and volatilization of the binder were the main causes of heat absorption.

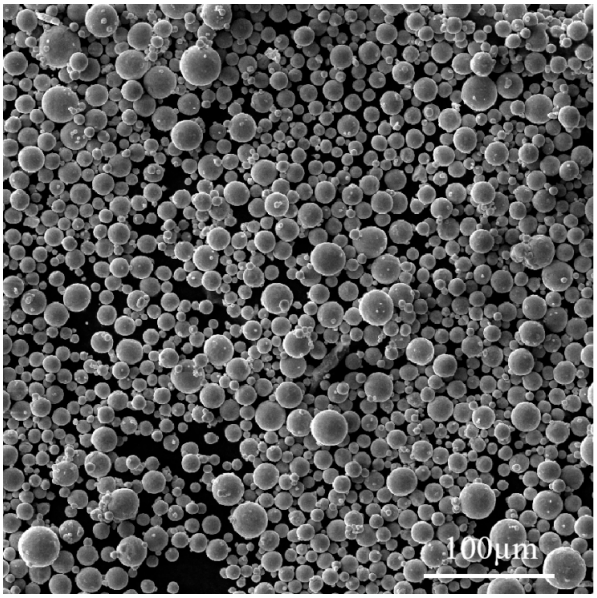



**Figure 1.** Morphology of Ti-6Al-4V powders shown by SEM.

**Table 1.** Distribution of particle size.

| | **Property Distribution of Particle Size (μm)** | | | |
|---|---|---|---|---|
| Powder | D10 | D50 | D90 | D97 |
| Ti-6Al-4V | 11.27 | 24.26 | 41.56 | 50.09 |

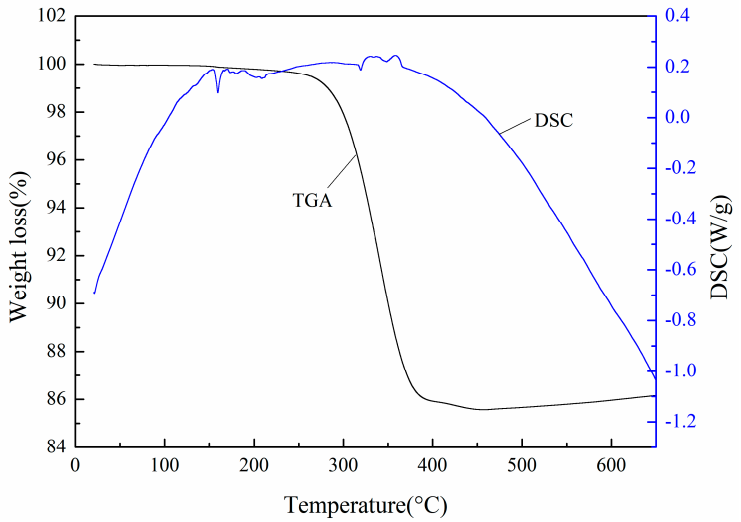



**Figure 2.** TGA of feedstock.

**Table 2.** Impurity contents (wt.%) of Ti-6Al-4V alloys.

| Mo | Fe | Y | C | H | N | O | Ti |
|---|---|---|---|---|---|---|---|
| 0.010 | 0.158 | 0.001 | 0.013 | 0.0031 | 0.010 | 0.090 | 0.001 |

The granular material was injected using a Battenfeld BA 250 CDC injection molding machine. The injection molding parameters were as follows: the injection pressure was 80 MPa, the holding pressure was 65 MPa, the injection speed was 50 mm/s and the injection temperature and mold temperature were 180 °C and 90 °C, respectively. The debinding stage can be divided into two steps, namely the first debinding step for removing low-molecular-weight polymer and the second debinding step for removing high-molecular-weight polymer [15]. In the first debinding step, the low-molecular-weight polymer is removed, and interconnected pore pathways are formed to facilitate the removal of the high-molecular-weight polymer in the second debinding step. In this study, the debinding stage was divided into catalytic and thermal debinding. Oxalic acid was used to remove the majority of the binders for 4.5 h at 130 °C. Then, drying took place in a 50 °C oven for 6 h. The final removal of the remaining binder and subsequent sintering were carried out in a single-step heat treatment run (Table 3). Sintering was performed in a vacuum of $10^{-5}$ mbar at 1150 °C, 1200 °C and 1250 °C, respectively, with a holding time of 4 h with 5 °C/min heating and cooling rates.

The C, N and O impurity contents of the sintered samples were determined with a conventional LECO analyzer (St. Joseph, MI, USA). The density of the as-sintered specimens was measured using the Archimedes method (average of five specimens). The relative sintered density can be calculated using Equation (1).

**Table 3.** The sintering profile of the Ti-6Al-4V structures.

| Step | Temperature (°C) | Heating Rate (°C/min) | Holding Time (min) |
|---|---|---|---|
| 1 | 250 | 5 | 0 |
| 2 | 375 | 2 | 30 |
| 3 | 450 | 2 | 60 |
| 4 | 600 | 5 | 30 |
| 5 | Maximum temperature | 5 | 240 |
| 6 | Room temperature | 5 | N/A |

$$\text{Relative sintered density} = \frac{\rho}{\rho_0} \quad (1)$$

where $\rho$ and $\rho_0$ are the apparent density of the specimen and the theoretical density of the MIM Ti-6Al-4V specimen, respectively. The theoretical density $\rho_0$ of MIM Ti-6Al-4V alloy was determined to be 4.42 g/cm$^3$ after measuring a sample exposed to hot isostatic pressing (HIP) treatment [29]. The specimens for microstructural investigation were taken from the cross-section of tensile specimens at the fracture area. The samples were polished and etched using Kroll's reagent (2.5 vol.% $HNO_3$ + 1.5 vol.% HCl + 1 vol.% HF + 95 vol.% $H_2O$) after grinding. The microstructures of the specimens were examined using a scanning electron microscope (SEM, Merlin, Zeiss, Jena, Germany) equipped with energy-dispersive spectroscopy (EDS, Octane Pro) detectors (Merlin, Zeiss, Jena, Germany). The tensile properties of the as-sintered specimens were determined in air at ambient temperature using an AGI-250KN testing machine (Shimadzu Instrument (Suzhou) Co., Ltd., Suzhou, China) with a traverse speed of 0.5 mm/min. The yield strength (YS), ultimate tensile strength (UTS) and elongation were calculated as the average values of five specimens under each sintering condition. All errors are reported as one standard deviation of the average tensile properties. The tensile test specimens were in the shape of a dog bone, manufactured by MIM, with a diameter of 5 mm and a gauge length of 65 mm.

## 3. Results and Discussion

### *3.1. Relative Densities and Impurity Levels*

Figure 3 shows the parts in the green and sintered stages. The green part showed significant shrinkage during the debinding and sintering process. The shrinkage after sintering was primarily due to the removal of a large amount of binder used in the injection of the samples and the densification of the part during the sintering process. The nominal length of the sintered compacts was between 80 and 80.5 mm with a typical thickness of about 5 mm.

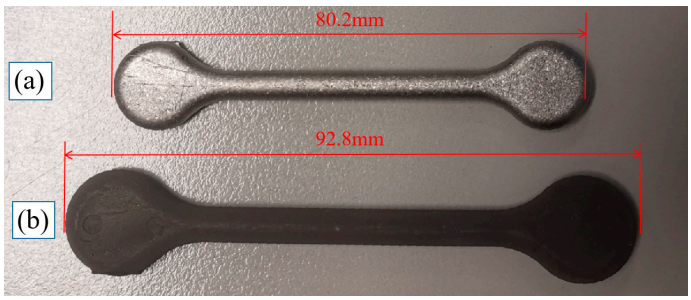



**Figure 3.** Appearance of parts in green and sintered stages: (**a**) as-sintered part; (**b**) green part.

Table 4 presents the apparent and relative sintered densities for specimens sintered at 1150 °C, 1200 °C and 1250 °C, calculated following Equation (1). The results show that the relative density of the sample increases with increasing sintering temperature [30].

**Table 4.** Relative density of sintered specimen.

| Sample | Temperature (°C) | Apparent Density (g/cm$^3$) | Relative Density (%) |
|---|---|---|---|
| 1 | 1150 | 4.316 | 97.647 |
| 2 | 1200 | 4.326 | 97.873 |
| 3 | 1250 | 4.328 | 97.919 |

Table 5 presents the impurity contents of the atomized powder, and the specimens after sintering at 1150 °C, 1200 °C and 1250 °C. The impurity contents are related to different parameters, such as starting powders, binder, specimens and processing parameters. After sintering at 1150 °C, 1200 °C and 1250 °C, compared with atomized powder, the N content of the specimens can be ignored, but the C and O contents increase significantly. The oxygen content for the specimens after sintering at 1150 °C, 1200 °C and 1250 °C are 0.287 wt.%, 0.288 wt.% and 0.323 wt.%, respectively. There are Increases in the oxygen content of about 1470 ppm, 1480 ppm and 1830 ppm, respectively, compared to the atomized powder. The carbon contents for the specimens after sintering at 1150 °C, 1200 °C and 1250 °C are 0.151 wt.%, 0.152 wt.% and 0.154 wt.%, respectively. There are increases in the carbon content of about 1370 ppm, 1380 ppm and 1400 ppm, respectively, compared to the atomized powder. The reason is that there is a reaction between the high-activity Ti alloy powder and the decomposed product of binders during the debinding and sintering. At higher sintering temperatures, the oxidation rate increases, resulting in higher O content in the specimens sintered at 1250 °C. The main influence of the impurity contents is on the mechanical properties of the sintering sample. High impurity contents result in higher strength, but lead to lower plastic elongation of the titanium component [31].

**Table 5.** Impurity levels of the atomized powder and debound and sintered specimen.

| Impurity | Atomized Powder (wt.%) | Sintered Specimen (wt.%) | | |
|---|---|---|---|---|
| | | 1150 °C | 1200 °C | 1250 °C |
| C | 0.014 | 0.151 | 0.152 | 0.154 |
| O | 0.140 | 0.287 | 0.288 | 0.323 |
| N | 0.013 | 0.016 | 0.016 | 0.017 |

### *3.2. Microstructure and Porosity*

Figure 4 shows SEM images of cross-sections of the tensile test specimens of Ti-6Al-4V sintered at 1150 °C, 1200 °C and 1250 °C, respectively. All the samples exhibit the typical microstructure of Ti-6Al-4V alloy irrespective of the sintering temperature. The microstructure consists of lamellar α/β colonies. The α-lamellae appear dark gray, while the β-phase between the α-lamellae is visible in a light gray color [31]. Moreover, the pores are visible as black dots. The existence of points in the microstructure of sintering may be related to incomplete debinding and removal of residual adhesives during the sintering process. However, it has been reported that points in the microstructure of Ti MIM components can lead to a decrease in tensile properties [32]. The shape of the pores sintered at 1150 °C (Figure 4a,b) is mainly rectangular, with a maximum size of 2 μm × 12 μm. At 1200 °C and 1250 °C, the shape of the pores is mainly circular, with a maximum diameter of 10 μm. However, the number of pores decreases with an increase in sintering temperature. This observation agrees with the relative density. The colony size was measured as 95 μm, 105 μm and 130 μm on average when the sintering temperature is 1150 °C, 1200 °C and 1250 °C, respectively.

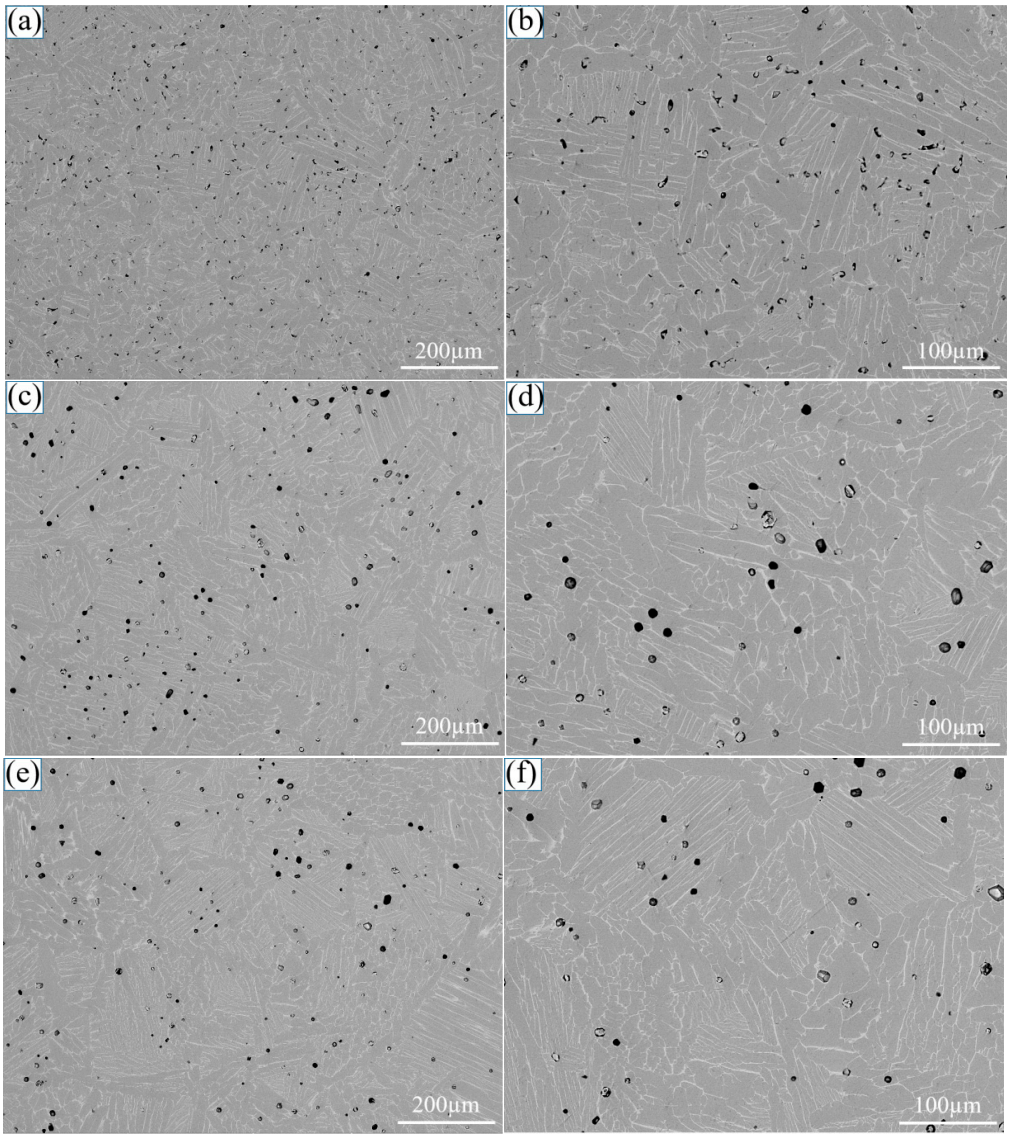



**Figure 4.** SEM images of cross-sections of the MIM-processed Ti-6Al-4V samples at different sintering temperatures: (**a**,**b**) 1150 °C; (**c**,**d**) 1200 °C and (**e**,**f**) 1250 °C.

### *3.3. Tensile Test Properties*

Figure 5 shows the statistical results of the room-temperature tensile properties of specimens at different sintering temperatures. The results of the tensile tests are also summarized in Table 6. The MIM-processed specimens sintered at 1150 °C show a yield strength (YS) of 896.35 MPa, an ultimate tensile strength (UTS) of 980.83 MPa and plastic elongation of 9.61%, which are similar values to the specimens sintered at 1200 °C (a yield strength of 877.23 MPa, an ultimate tensile strength of 981.92 MPa and plastic elongation of 7.74%). When the sintering temperature is 1250 °C, it leads to a significantly higher yield strength of 923.33 MPa, an ultimate tensile strength of 1002.24 MPa and low plastic elongation of 6.57%. The tensile properties of Titanium alloys produced by powder technology are determined by the alloying elements and their contents, impurity contents, relative sintered density and microstructure [33]. The yield and ultimate tensile strengths generally increase with an increase in relative sintered density (decreasing porosity) and with an increase in the impurity content [33]. The lower the porosity in MIM, the better the yield strength and ultimate tensile strength [34], which was the case in this work. On the other hand, Bian et al. obtained higher yield stress and ultimate tensile stress due to a high content of O [27]. In their work, Ti-6Al-V alloy samples with 4000 ppm oxygen were fabricated through metal

injection molding, and a significantly higher yield strength of 905 ± 10 MPa and ultimate tensile strength of 960 ± 20 MPa were obtained. In this work, the higher density of the specimen and impurity contents are the main reasons for the better mechanical properties of the sintered specimen [35]. However, in this work, it is suggested that sintering at a lower temperature on MIM-processed Ti-6Al-4V can obtain better comprehensive mechanical properties, which is in accordance with the investigations of other scholars [27]. The reason is that the microstructure became coarse because of sintering at higher temperatures, which might have deteriorated the plastic elongation.

**Table 6.** Average tensile properties of sintered specimens at different temperatures.

| Sample | Temperature (°C) | UTS (MPa) | YS (MPa) | Elongation (%) |
|---|---|---|---|---|
| 1 | 1150 | 980.83 ± 2 | 896.35 ± 5 | 9.61 ± 0.2 |
| 2 | 1200 | 981.92 ± 2 | 877.23 ± 5 | 7.74 ± 0.2 |
| 3 | 1250 | 1002.24 ± 2 | 923.33 ± 5 | 6.57 ± 0.2 |

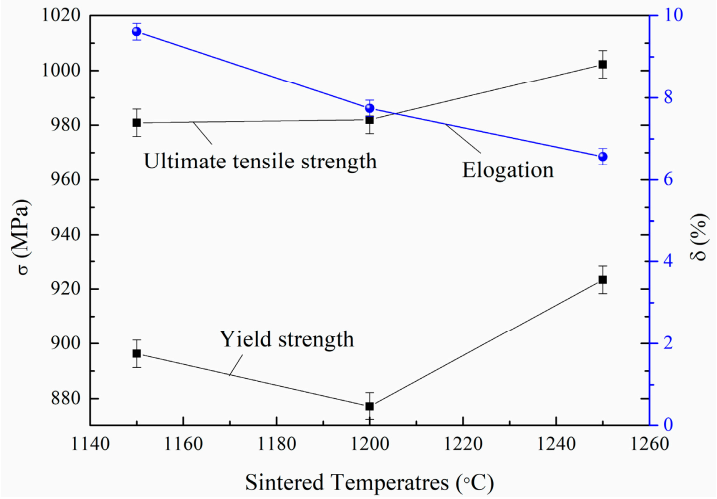



**Figure 5.** The results of the room-temperature tensile properties of the specimens at different sintering temperatures.

Figure 6 shows the fractography of the specimens after sintering at 1150 °C, 1200 °C and 1250 °C. At the sintering temperature of 1150 °C, there are larger dimples on the tensile fracture surface, which indicates ductile fracture with improved plasticity (Figure 6a). When the sintering temperature is 1200 °C, there are a few dimples, indicating localized plastic deformation during the tensile test, which corresponds to a quasi-cleavage fracture with relatively poor plasticity, consistent with its mechanical properties (Figure 6b). When the sintering temperature is 1250 °C, the fracture surface of the specimen reveals a smooth, wave-like structure, indicating the characteristic of brittle fracture behavior (Figure 6c) [8]. Figure 6 also shows voids on the fracture surfaces, regardless of the sintering temperature. However, as the sintering temperature increases, the pores in the specimens decrease markedly.

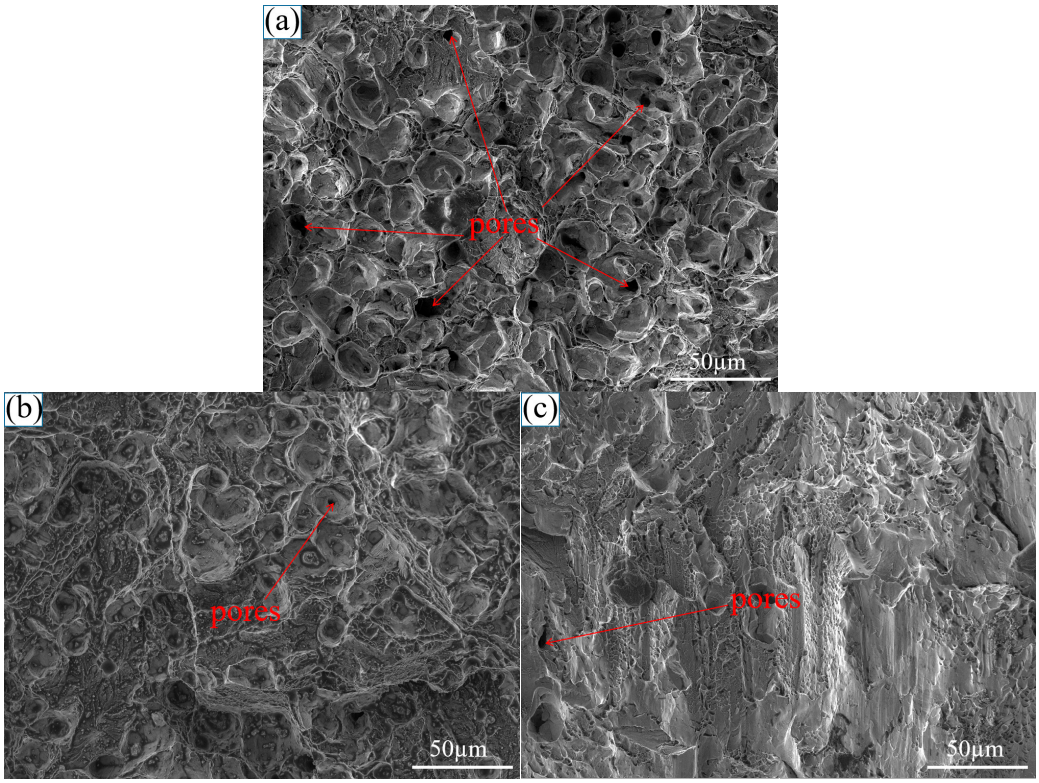



**Figure 6.** SEM micrographs of fracture surface at (**a**) 1150 °C; (**b**) 1200 °C; and (**c**) 1250 °C.

## 4. Conclusions

Herein, the influences of sintering temperatures on the microstructure and mechanical properties of Ti-6Al-4V alloy fabricated through MIM were investigated at sintering temperatures of 1150 °C, 1200 °C and 1250 °C. The conclusions were as follows:

1. The relative density of MIM-processed Ti-6Al-4V alloys increases with an increase in sintering temperature, and a maximum relative density of 97.919% is achieved at 1250 °C.
2. The oxygen contents of the specimens after sintering at 1150 °C, 1200 °C and 1250 °C are 0.287 wt.%, 0.288 wt.% and 0.323 wt.%, respectively.
3. The microstructure consists of lamellar α/β colonies and black dots, and the number of pores decreases with an increase in sintering temperature. The colony size increases with increasing sintering temperature.

When the sintering temperature is 1250 °C, it leads to a significantly higher yield strength of 923.33 MPa, an ultimate tensile strength of 1002.24 MPa and low plastic elongation of 6.57%. However, when the sintering temperature is 1150 °C, the MIM-processed specimen exhibits better comprehensive mechanical properties for Ti-6Al-4V alloy, with a 896.35 MPa yield strength, a 980.83 MPa ultimate tensile strength and 9.61% plastic elongation. The reason is that the microstructure of Ti-6Al-4V alloy is finer and the oxygen content is lower.

**Author Contributions:** Conceptualization, Z.M. and Y.S.; methodology, Y.S.; software, Y.M.; validation, C.Z. (Changjiang Zhang), H.W. and L.X.; formal analysis, H.W.; investigation, C.Z. (Changjiang Zhang); resources, H.W.; data curation, Z.M.; writing—original draft preparation, Y.S.; writing—review and editing, Y.S.; visualization, Z.M.; supervision, C.Z. (Chuancang Zhou); project administration, Y.S.; funding acquisition, Y.S. and H.W. All authors have read and agreed to the published version of the manuscript.

**Funding:** This research were financially supported by the China Scholarship Council (NO. 202308330254) and Lishui Science and Technology Bureau (NO. 2024GYX03).

**Data Availability Statement:** Data are contained within the article.

**Conflicts of Interest:** Haiyang Wang is employed by Jiangsu Jinwu New Materials Co., Ltd. The remaining authors declare that the research was conducted in the absence of any commercial or financial relationships that could be construed as a potential conflict of interest.

## References

1. Ye, Q.; He, G. In-situ formed graded microporous structure in titanium alloys and its effect on the mechanical properties. *Mater. Des.* **2015**, *83*, 295–300. [CrossRef]
2. Fu, Y.L.; Guo, N.; Zhou, L.; Cheng, Q.; Feng, J.C. Underwater wire-feed laser deposition of the Ti-6Al-4V titanium alloy. *Mater. Des.* **2020**, *186*, 108284. [CrossRef]
3. Kaouka, A.; Benarous, K. Electrochemical boriding of titanium alloy Ti-6Al-4V. *J. Mater. Res. Technol.* **2019**, *8*, 6407–6412. [CrossRef]
4. Mirnov, S.; Sato, Y.S.; Kokawa, H. Friction-stir welding and processing of Ti-6Al-4V titanium alloy: A review. *J. Mater. Sci. Technol.* **2018**, *34*, 58–72. [CrossRef]
5. Zhang, C.J.; Yang, Z.B.; Qu, B.L.; Lian, Q.H.; Guo, R.P.; Zhang, S.Z.; Kong, F.T.; Cao, P. Superior strength-ductility synergy in a nera-α titanium alloy fabricated by severe plastic deformation at lower temperatures. *Scripta. Mater.* **2024**, *248*, 116140. [CrossRef]
6. Suwanpreecha, C.; Songkuea, S.; Wangjina, P.; Tange, M.; Pongsaksawad, W.; Manonukul, A. Effect of Mo Additions on the physical, Mechanical and Corrosion Properties of Commercially Pure Ti Fabricated by Metal Injection Moulding. *Met. Mater. Int.* **2023**, *29*, 3298–3316. [CrossRef]
7. Childerhouse, T.; Jackson, M. Near net shape manufacture of titanium alloy components from powder and wire: A review of state-of-the-art process routes. *Metals* **2019**, *9*, 689. [CrossRef]
8. Ren, W.L.; Chen, X.L.; Zhao, B.S.; Dan, Z.H.; Li, Y.H.; Chang, H.; Zhou, Z.F. Investigating evolution of microstructures and mechanical properties in metal injection molding Ti6Al4V with sintering processing by quasi in-situ strategy. *Powder Technol.* **2024**, *439*, 119694. [CrossRef]
9. Dehghan-Manshadia, A.; Bermingham, M.J.; Dargusch, M.S.; StJohn, D.H.; Qian, M. Metal injection moulding of titanium and titanium alloys: Challenges and recent development. *Powder Technol.* **2017**, *319*, 289–301. [CrossRef]
10. Thavanayagam, G.; Swan, J.E. Aqueous debinding of polyvinyl butyral based binder system for titanium metal injection moulding. *Powder Technol.* **2018**, *326*, 402–410. [CrossRef]
11. Sim, K.H.; Wang, G.F.; Son, R.C.; Choe, S.L. Influence of mechanical alloying on the microstructure and mechanical properties of powder metallurgy Ti2AlNb-based alloy. *Powder Technol.* **2017**, *317*, 133–141. [CrossRef]
12. Ergül, E.; Özkan Gülsoy, H.; Günay, V. Effect of sintering parameters on mechanical properties of injection moulded Ti-6Al-4V alloys. *Powder Metall.* **2009**, *52*, 65–71. [CrossRef]
13. Suwanpreecha, C.; Manonukul, A. Review: Fatigue Properties of Ti-6Al-4V Alloys Fabricated by Metal Injection Moulding. *SIAM Sci. Innov. Adv. Mater.* **2021**, *1*, 64005.
14. Lim, K.; Hayat, M.D.; Jena, K.D.; Zhang, W.; Cao, P. On amine treated polyoxymethylene (POM) blends with low formaldehyde emission for metal injection moulding (MIM). *J. Mater. Sci.* **2022**, *57*, 15160–15170. [CrossRef]
15. Suwanpreecha, C.; Manonukul, A. A Review on Material Extrusion Additive Manufacturing of Metal and How It Compares with Metal Injection Moulding. *Metals* **2022**, *12*, 429. [CrossRef]
16. Dehghan-Manshadi, A.; Yu, P.; Dargusch, M.; StJohn, D.; Qian, M. Metal injection moulding of surgical tools, biomaterials and medical devices: A review. *Powder Technol.* **2020**, *364*, 189–204. [CrossRef]
17. Bootchai, N.; Taweejun, N.; Manonukul, A.; Kanchanomai, C. Metal injection moulded titanium: Mechanical properties of debinded powder and sintered metal. *J. Mater. Eng. Perform.* **2020**, *29*, 4559–4568. [CrossRef]
18. Lim, K.A.; Hayat, M.D.; Jena, K.D.; Yuan, Z.T.; Li, L.; Cao, P. Formulating titanium powder feedstocks for metal injection moulding from a clean binder system. *Powder Technol.* **2024**, *433*, 119214. [CrossRef]
19. Xu, P.; Pyczak, F.; Limberg, W.; Willumeti-Rmer, R.; Ebel, T. Superior Fatigue Endurance Exempt from High Processing Cleanliness of Metal-Injection-Molded β Ti-Nb-Zr for Bio-tolerant Applications. *Mater. Des.* **2021**, *211*, 110141. [CrossRef]
20. Mahmud, N.N.; Azam, F.A.A.; Ramli, M.I.; Foudzi, F.M.; Sulong, A.B. Rheological properties of irregular-shaped titanium-hydroxyapatite bimodal powder composite moulded by powder injection molding. *J. Mater. Res. Technol.* **2021**, *11*, 2255–2264. [CrossRef]
21. Moghadam, M.S.; Fayyaz, A.; Ardestani, M. Fabrication of titanium components by low-pressure powder injection moulding using hydride-dehydride titanium powder. *Powder Technol.* **2021**, *377*, 70–79. [CrossRef]
22. Royer, A.; Barriere, T.; Gelin, J.C. Development and characterisation of a metal injection molding bio sourced inconel 718 feedstokc based on polyhydroxyakanoates. *Metals* **2016**, *6*, 89. [CrossRef]

23. Ferri, O.M.; Ebel, T.; Bormann, R. High cycle fatigue behavior of Ti-6Al-4V fabricated by metal injection moulding technology. *Mater. Sci. Eng. A* **2009**, *504*, 107–113. [CrossRef]
24. Guo, S.B.; Qu, X.H.; He, X.B.; Zhou, T.; Duan, B.H. Powder injection molding of Ti-6Al-4V alloy. *J. Mater. Process. Technol.* **2006**, *173*, 310–314.
25. Rane, K.K.; Date, P.P.; Kotwal, G.N.; Nayak, K.C.; Srivatsan, T.S. Influence of sintering on mechanical response of metal injection moulded parts. *Mater. Manuf. Process.* **2023**, *38*, 1694–1706. [CrossRef]
26. Mohamad Nor, N.H.; Muhamad, N.; Mohd Ihsan, A.K.A.; Jamaludin, K.R. Sintering Parameter Optimization of Ti-6Al-4V Metal Injection Molding for Highest Strength Using Palm Stearin Binder. *Procedia Eng.* **2013**, *68*, 359–364.
27. Obasi, G.C.; Ferri, O.M.; Ebel, T.; Bormann, R. Influence of processing parameters on mechanical properties of Ti-6Al-4V alloy fabricated by MIM. *Mater. Sci. Eng. A* **2010**, *527*, 3929–3935. [CrossRef]
28. Wang, J.H.; Shi, Q.N.; Wu, C.L.; Xi, J. Rheological characteristics of injection molded titanium alloys powder. *Trans. Nonferrous Met. Soc. China* **2013**, *23*, 2605–2610. [CrossRef]
29. Limberg, W.; Willumeit-Römer, R.; Pyczak, F.; Ebel, T.; Stark, A. Enhancement of Fatigue-Properties of MIM-Processed Ti-6Al-4V by Addition of Yttrium and Characterization by In Situ X-Ray Scattering. In Proceedings of the Euro PM2017 Congress & Exhibition, Milan, Italy, 1–4 October 2017.
30. Zhang, H.M.; He, X.B.; Qu, X.H.; Zhao, L.M. Microstructure and mechanical properties of high Nb containing TiAl alloy parts fabricated by metal injection molding. *Mater. Sci. Eng. A* **2009**, *526*, 31–37. [CrossRef]
31. Wen, G.; Cao, P.; Gabbitas, B.; Zhang, D.; Edmonds, N. Development and design of binder systems for titanium metal injection molding: An overview. *Metall. Mater. Trans. A* **2012**, *44*, 1530–1547. [CrossRef]
32. Chong, Y.; Bhattacharjee, T.; Tsuji, N. Bi-lamellar microstructure in Ti-6Al-4V: Microstructure evolution and mechanical properties. *Mater. Sci. Eng. A* **2019**, *762*, 138077. [CrossRef]
33. Subasi, M.; Safarian, A.; Karatas, C. The investigation of production parameters of Ti-6Al-4V component by powder injection molding. *Int. J. Adv. Manuf. Technol.* **2019**, *105*, 4747–4760. [CrossRef]
34. Ebel, T. *Handbook of Metal Injection Molding*; Woodhead Publishing: Cambridge, UK, 2012; pp. 415–445.
35. Bian, T.; Ding, C.; Yao, X.; Wang, J.; Mo, W.; Wang, Z.; Yu, P.; Ye, S. Mechanisms of heat treatment and ductility improvement of high-oxygen Ti-6Al-4V alloys fabricated by metal injection molding. *Mater. Sci. Eng. A* **2022**, *840*, 142924. [CrossRef]


**Disclaimer/Publisher's Note:** The statements, opinions and data contained in all publications are solely those of the individual author(s) and contributor(s) and not of MDPI and/or the editor(s). MDPI and/or the editor(s) disclaim responsibility for any injury to people or property resulting from any ideas, methods, instructions or products referred to in the content.